# Is Reducibility in Nuclear Multifragmentation related to Thermal Scaling ? ⋆

A. Wieloch [a,1], E. Plagnol [d], D. Cussol [a], J. Péter [a], M. Assenard [f], G. Auger [c], Ch.O. Bacri [d], F. Bocage [a], B. Borderie [d], R. Bougault [a], R. Brou [a], Ph. Buchet [b], J.L. Charvet [b], A. Chbihi [c], J. Colin [a], R. Dayras [b], A. Demeyer [e], D. Doré [d,2], D. Durand [a], P. Eudes [f], J.D. Frankland [d], E. Galichet [e], E. Genouin-Duhamel [a], E. Gerlic [e], M. Germain [f], D. Gourio [f,3], D. Guinet [e], F. Gulminelli [a], P. Lautesse [e], J.L. Laville [f], J.F. Lecolley [a], A. Le Fèvre [c], T. Lefort [a], R. Legrain [b], O. Lopez [a], M. Louvel [a], L. Nalpas [b], A.D. Nguyen [a], M. Parlog [h], G. Politi [c], A. Rahmani [f], T. Reposeur [f], M.F. Rivet [d], E. Rosato [g], F. Saint-Laurent [c,4], S. Salou [c], J.C. Steckmeyer [a], M. Stern [e], G. Tabacaru [h], B. Tamain [a], L. Tassan-Got [d], O. Tirel [c], E. Vient [a], C. Volant [b], J.P. Wieleczko [c].

[a] *LPC Caen (IN2P3-CNRS/ISMRA et Université), 14050 Caen Cedex , France*

[b] *CEA DAPNIA-SPhN, C.E. Saclay, 91191 Gif-sur-Yvette Cedex, France*

[c] *GANIL (DSM-CEA/IN2P3-CNRS), B.P. 5027, 14076 Caen Cedex 5, France*

[d] *IPN Orsay (IN2P3-CNRS), 91406 Orsay Cedex, France*

[e] *IPN Lyon (IN2P3-CNRS/Université), 69622 Villeurbanne Cedex, France*

[f] *SUBATECH (IN2P3-CNRS/Université), 44070 Nantes Cedex, France*

[g] *Dipartimento di Scienze Fisiche, Univ. di Napoli,180126 Napoli, Italy.*

[h] *Nuclear Institute for Physics and Nuclear Engineering, Bucharest, Romania*

**Abstract**

Thermal scaling (Arrhenius law for an "elementary" probability $p$ of binomial function) and reducibility in intermediate mass fragments (IMF's) production are examined for data of the reaction $^{129}$Xe+$^{nat}$Sn at 50 MeV/u. The study of the longitudinal velocities and of the average transverse energies of the IMF's contradicts the assumption that the total transverse energy of all detected particles $E_t$ is related to a well defined temperature. The separation of $E_t$ into the total transverse energy of light charged particles (Z=1,2) and that of IMF's elucidates the algorithm which induces a linear behavior of $log(1/p)$ vs $1/\sqrt{E_t}$. Even in the case of a single thermalized source, calculations based on a sequential statistical model show that the Arrhenius

law cannot be observed if $E_t$ is taken as an estimation of the thermal energy.

---

## 1 Introduction.

In heavy ion collisions at intermediate energy ($>$ 20 MeV/u), the production of several Intermediate Mass Fragments (IMF's, usually defined as nuclei with atomic number $3 \leq Z \leq 20$), becomes an important reaction channel. These IMF's are apparently produced over the whole range of impact parameters and, for the most violent collisions, their total mass can sum up to half the mass of the entire system and they exhaust a significant fraction of the available energy. This important decay mode is not yet well understood and suggestions concerning their origin range from dynamical effects [1–3] to purely statistical processes [4–6], depending on the impact parameter range considered.

An interesting attempt at a global, impact parameter independent, understanding has been suggested by L.G.Moretto and co-workers [7–9]. They argue that IMF production could be reducible to an elementary thermal process. The probability $p$ for this elementary process-emission is defined through the binomial function:

$$P_n^m(p) = \frac{m!}{n!(m-n)!} p^n (1-p)^{m-n} \tag{1}$$

where $m$ denotes the number of attempts undertaken by a system to emit a fragment, $p$ the probability for its emission, and $n$ the number of emitted IMF's ($n \equiv N_{IMF}$).

Furthermore, these authors [7–9] claim that such elementary processes are thermal in nature. This statement is based on the observation that $log(1/p)$ is a linear function of the inverse square root of the total transverse energy, $E_t$, calculated for all detected charged particles and fragments:

$$p \sim e^{-B/\sqrt{E_t}}. \tag{2}$$

Assuming that $E_t$ is proportional to the thermal excitation energy ($E^*$) of the system and using the Fermi gas model relation between temperature $T$ and $E^*$ ($T \sim \sqrt{E_t}$), one obtains the Arrhenius law (thermal scaling) by replacing $\sqrt{E_t}$ by T in eq. 2. The slope, $B$, is interpreted as the mean barrier for IMF emission **[8,9]**.

This interpretation of the experimentally observed Arrhenius-type law for IMF production versus $\sqrt{E_t}$ has been criticized on several grounds. A general criticism comes from the

---

⋆ Experiment performed at Ganil

[1] on leave of absence from Institute of Physics, Jagiellonian University, Reymonta 4, 30059 Kraków, Poland.

[2] present address : CEA DAPNIA/SPhN, CE Saclay, 91191 Gif-sur-Yvette, France

[3] present address : GSI, Postfach 110552, 64220 Darmstadt, Germany

[4] present address : CEA, DRFC/STEP, CE Cadarache, 13108 Saint-Paul-lez-Durance, France

observation that, as a function of impact parameter, several "sources" of emission exist and that their relative importance varies with the impact parameter **[1,10–18]** . In this case, the definition of a unique temperature is problematic and has to be justified.

Another critical comment made recently [19] is related to the relationship between the temperature and the experimentally measured transverse energy. The extraction of parameters $p$ and $m$ is related not only to the mean value of the IMF probability distribution (for a given $T$) but also to the width (fluctuation). Any modification (increase) of this width due to the use of a substitution parameter (ie $\sqrt{E_t}$ instead of $T$) should significantly modify the Arrhenius behavior. Other critics argue that charge conservation should diminish the observed widths and that furthermore the observed Arrhenius behavior is essentially a signature of the linear dependence of $E_t$ on the IMF multiplicity [20]. **It has also been shown in [21] that the observed binomial-like light particle multiplicity distributions do not necessarily imply the evidence of reducibility to an elementary binary emission probability.**

The purpose of this article is to present new experimental data related to these questions and to check the thermal assumption by using the kinematical analysis of these IMF's: what are their velocity distribution, how do they relate to different sources and what is their influence on the measurement of $E_t$ ? We conclude that indeed the thermal hypothesis cannot be sustained.

## 2 Experimental results and discussion.

The data used in the present analysis come from the study of the $^{129}$Xe+$^{nat}$Sn system with the INDRA detector at GANIL for incident energies ranging from 25 to 50 MeV/u. These nuclei are heavy enough to provide a large number of IMF's but not so heavy that fission is an important channel. The description of the apparatus and the conditions in which the experiment was performed can be found in [1,22]. The main features of these reactions are described in [1,10–18], especially the dominant role of binary dissipative collisions (quasi-projectile, QP, and quasi-target, QT) accompanied by mid-rapidity emission (pre-equilibrium or neck emission), except in very central collisions where an incomplete fusion nucleus may be formed [5,13].

With respect to the present questions, it is important to point out that the experimental set-up was very efficient ($90\%$) for the detection of the light particles and the IMF's. The most noticeable inefficiencies are related to the non-detection of the forward peaked ($\Theta_{Lab} \leq 2^o$) QP residue and of the very slow QT residue. To diminish the influence of these deficiencies on the measured $E_t$, only events where $> 60\%$ of the total parallel momentum has been measured were considered. We checked that this selection has no influence on the results. When present, the influence of the QP and QT residues on $E_t$ was checked to

be negligible in all instances.

In these events, the charged particle multiplicity varies from 2 for peripheral collisions up to ≈40 for central ones. Since most of the reaction cross section is essentially binary, special care was taken in identifying the QP residue which is present in each event. In peripheral and semi-central collisions this residue has a charge greater than the upper limit of the IMF definition. When it has a smaller charge ($Z \leq 20$), it is removed from the IMF distribution. Strictly speaking the same problem arises for the QT source but in most cases the heaviest residue is automatically removed since its kinetic energy is below the detection thresholds. Note that in refs [7–9], both the QP and the QT residues were removed by the detection thresholds. In our case the QP residue has to be eliminated in the analysis.

In the present analysis we extracted the elementary probability $p$, and the number of drawings $m$ of the binomial function, from the two relations:

$$p = 1 - \frac{\sigma^2}{< N_{IMF} >}, \tag{3}$$

$$m = \frac{< N_{IMF} >}{1 - \frac{\sigma^2}{< N_{IMF} >}}, \tag{4}$$

where $\sigma^2$ and $< N_{IMF} >$ are the measured variance and mean value of the IMF multiplicity distribution for any given transverse energy, respectively.

Figures 1 a,c show $p$ and $m$ as a function of $1/\sqrt{E_t}$. All detected charged particles have been taken into account for the calculation of $E_t$. The Arrhenius-type law is indeed well observed and the parameter $m$ is roughly constant with a value of 10. This constancy of $m$ is itself surprising and its interpretation in terms of a thermal picture is not straightforward.

In figure 2, the parallel velocity of the IMF's are shown for different bins of $E_t$. The solid curve corresponds to the case when the heaviest product was eliminated in each event while for the dashed curve the heaviest product was taken into account (if within the IMF definition). The position and the width of the broad arrow indicate the mean and the FWHM of the velocity distribution of the QP residue. As was shown in ref [1], only a portion of these IMF's originates from a well defined projectile (target) like source. In fact, most come from an imprecisely defined intermediate velocity region. This is particularly clear for small $E_t$ (most peripheral) collisions where the QP residue velocities are measured with precision. In the same figure the black circles and the right-hand scale correspond to the average transverse energy for Z=2 particles for each parallel velocity bin. It has been shown in figure 3 of reference [18] that for particles thermally emitted by a single source, such a plot exhibits a maximum around the source parallel velocity. For each $E_t$ bin, it is clearly seen that the average transverse energies in the intermediate velocity

region is different from those of the QP and QT velocity regions. Thus, even in case of thermally driven emissions, the temperatures of the different sources are different. A clear understanding of the origin of these IMF's has yet to be achieved and is beyond the scope of this paper. Whatever the exact scenario, the kinematical properties of the IMF's do not point to a thermal emission with a well defined temperature for the whole system and puts in serious doubt the assumed relation between $E_t$ and whatever temperature can be defined. Similar results have also been observed for other systems [2,3,18] and seem to be a general feature of intermediate energy heavy ion collisions.

A remarkable confirmation of this is found in figure 3a where the mean total transverse energy, $< E_{t,IMF} >$, of the IMF's is plotted as a function of the total transverse energy, $E_{t,LCP}$, of the light particles, for IMF multiplicities ranging from 1 to 9. For a given IMF number, the IMF transverse energy is quite independent of the LCP transverse energy. Furthermore, the transverse energy carried away by the IMFs is proportional to the number of IMF's, each IMF carrying an average transverse energy of 30 MeV. This indicates that the IMF production mechanism is not very sensitive to the temperature of the system as estimated via $E_{t,LCP}$.

Figure 3b shows that this behavior extends beyond the mean value and that the shape of the IMF's transverse energy ($e_{t,IMF}$) distribution itself is quite invariant as a function of IMF multiplicity. It has been checked that this invariance is also observed as a function of $E_{t,LCP}$.

We can now study the behavior of $1/p$ and $m$ as a function of the various ingredients of $E_t$. In a first step, we study the value of these parameters as a function of $E_{t,LCP}$ : fig. 1b and d, full squares. As one can see, this dependence is highly non-linear for both $1/p$ and $m$. Moreover, for $1/\sqrt{E_{t,LCP}} > 0.05$ the variance, $\sigma^2$, becomes greater than the average value $< N_{IMF} >$, so in eq. 3 and 4 the binomial parameters $p$, $m$ become negative. We have taken the absolute values of $1/p$ and $m$ in order to present this region: open squares in fig. 1 b,d. The functional dependences of $|1/p|$ and $|m|$ are very similar. This is typical of induced decorrelation and was noticed in numerical simulations[19].

In the next step, the transverse energy carried by IMF's was taken into account, but the observed mean value was used instead of the actual individual value:

$$E_{t,30} = E_{t,LCP} + 30MeV * N_{IMF}, \tag{5}$$

where 30 MeV corresponds to the mean transverse energy of IMF which is, as seen in fig. 3a, independent on IMF's multiplicity and on $E_{t,LCP}$. For $N_{IMF} = 0$ the present and previous values of $E_t$ are identical; for $N_{IMF} = 1$ the current formula displaces the transverse energy value obtained with the previous prescription by 30 MeV; for $N_{IMF} = 2$ the displacement is 60 MeV, and so on. The result is presented as full triangles in fig. 1 b,d. As one can see now $\log(1/p)$ is a linear function of $1/\sqrt{E_{t,30}}$ in the whole range of

$E_{t,30}$. $m$ does not exhibit any discontinuity anymore, but is decreasing exponentially with $E_{t,30}$.

Finally, instead of taking the average transverse energy of an IMF, one can use a value chosen randomly according to the experimental distribution. Then one produces $E_{t,ran}$, which can be used in the following relation:

$$E_{t,r} = E_{t,LCP} + E_{t,ran} * N_{IMF} \quad (6)$$

with $< E_{t,ran} >= 30MeV$. The difference with equation (5) is due to additional fluctuations associated with $N_{IMF}$. As a result of these fluctuations the slope of the linear behavior of $\log(1/p)$ vs $1/\sqrt{E_{t,ran}}$ has increased with respect to the previous approach: fig. 1 b, full stars. This last prescription gives a result very similar to the direct experimental result: solid line reproducing the one of fig. 1 a. The same conclusion applies to $m$.

**This analysis leads us to consider** that the total transverse energy **cannot be** correlated to the thermal energy **of the whole system, because this global thermal energy cannot be defined**. $E_t$ **results from the contributions of LCP's and IMF's** which are emitted from different sources with different temperatures if a thermally driven emission is assumed, or emitted via a non-equilibrium process if dynamical effects are present **(figure 2)**.

In fact both $p$ and $E_t$ depend on $E_{t,IMF}$. This auto-correlation produces a behavior of $\log(1/p)$ versus $1/\sqrt{E_t}$ which depends on **the values of** $< e_{t,IMF} >$**, the IMF's mean tranverse energy, relative to** $< e_{t,LCP} >$**, the LCP's mean transverse energy: a linear behavior is obtained if** $< e_{t,IMF} >$ **is larger than** $< e_{t,LCP} >$ **[23]. This condition is fulfilled in the experiment in which** $< e_{t,IMF} >= 30MeV$ **and** $< e_{t,IMF} >= 14MeV$**. The algorithm which leads to a linear behavior is described in detail in ref. [23].**

## 3 Simulation of a statistically decaying single source.

To test the hypothesis of thermal scaling in a system where thermal equilibrium is achieved, the following simulation was performed. A single source with $Z = 54$, $A = 129$ and thermal excitation energy $E^*$ was subjected to **sequential** decay according to the transition state method ($Z > 2$) and Hauser-Feschbach formalism ($Z \leq 2$) as implemented in the SIMON code [24]. The temperature was related to the excitation energy via the usual Fermi gas relationship: $E^* = a.T^2$. The value of $E^*$ was varied randomly from 1 to 12 MeV/u. A large number ($\approx 3 * 10^5$) of events were generated and analyzed on an event-by-event basis. As in the data analysis, the heaviest product (residue) was removed in each event and IMF's were defined as the remaining fragments with $3 \leq Z \leq 20$.

Two approaches were used to estimate the initial temperature of the system. In the first one (figure 4, open diamonds) the true thermal excitation energy $E^*$ was used : the abscissa is then $1/\sqrt{E^*}$. One observes a broad region of excitation energy (up to 7 MeV/u) where $log(1/p)$ decreases almost linearly with $1/\sqrt{E^*}$ (i.e. $1/T$), as in the Arrhenius law. Above 7 MeV/u ($E^* = 900$ MeV) one observes a gradual increase. This is due to the finite size of the system and has been also observed in MMMC model calculations (statistical simultaneous scenario of charged fragment production) [4]. The value of $m$ increases with increasing excitation energy $E^*$, whereas it is found almost constant in the experiment (fig. 1c).

In the second approach (figure 4, dots and open circles), one assumes a linear correlation between $E_t$, the transverse energy of all emitted charged particles and fragments, and $E^*$: the abscissa is then $1/\sqrt{E_t}$. As in fig. 1 b,d, open circles correspond to the region where the parameters of the binomial law $p$ and $m$ become negative. The signal produced by this approach is completely different from the Arrhenius law and shows a strong **divergence**. To complete the comparison with the data, the squares in fig. 4 correspond to the case where only the total transverse energy of LCP's was used ($1/\sqrt{E_x} = 1/\sqrt{E_{t,LCP}}$). The points are shifted to lower values of $1/\sqrt{E_x}$, but the shape is the same. Since in the experiment the total detected mass is larger than that of $^{129}$Xe, we have also made calculations for heavier systems. The values of $1/\sqrt{E_x}$ where $p$ and $m$ become negative are shifted, but the shape, and the conclusions, are not modified. It appears thus that the assumption of this approach does not preserve the Arrhenius behavior and that temperature is not proportional, on an event by event basis, to the square root of the total transverse energy (and neither to the transverse energy of LCP's). This results in quite broad excitation energy (temperature) fluctuations **and widths broadening of the IMF's distributions** for each bin in transverse energy. Similar conclusions were reached recently in [19].

## 4 Conclusion.

Both the experimental measurement of the IMF velocity (fig. 2, [1]) and the observed trend of the transverse energy associated to Z=2 particles and to IMFs (figs. **2 and** 3) give evidence that the assumption that $\sqrt{E_t}$ is proportional to a well determined temperature $T$ of the whole system is not supported by experimental facts. The analysis of a thermal statistical model calculation shows clearly that the use of $E_t$ instead of $T$ destroys the initial Arrhenius-type behavior : a binning of events according to $E_t$ is not equivalent, in terms of fluctuations, to a binning according to $T$. In this simulation, the inclusion, or not, of the IMF transverse energy only displaces the divergency observed but does not cure it. On the contrary, the experimental data show that the linear behavior is critically due to the IMF contribution. The study of the algorithm which induces linearity by including IMF's [23] makes it possible to conclude that this linearity is not a signature of a thermal process. A better understanding of IMF emission should be looked for in a

thorough study of their dynamical properties, in order to separate "dynamically emitted IMF's" from those statistically emitted from thermal sources.

## References


[1] J. Łukasik et al., Phys. Rev. C **55** (1997) 1906.

[2] J. Tõke et al., Phys. Rev. Lett. **77** (1996) 3514.

[3] J.Dempsey et al. Phys. Rev. C **54** (1996) 1710

[4] A.S. Botvina, D.H.E. Gross, Phys. Lett. B **344** (1995) 6.

[5] N.Marie et al. Phys. Lett. B **391** (1997) 15.

[6] R.Bougault et al. XXXV Int. Winter Meeting on Nuclear Physics, Bormio (Italy), Feb 3-7, 1997, edited by I.Iori.

[7] L.G. Moretto et al., Phys. Rev. Lett. **74** (1995) 1530.

[8] K. Tso et al., Phys. Lett. B **361** (1995) 25.

[9] L.G. Moretto et al., Phys. Rep. **287** (1997) 249.

[10] G. Rudolf et al., Phys. Lett. B **307** (1993) 287.

[11] J.F. Lecolley et al., Phys. Lett. B **354** (1995) 202.

[12] A. Kerambrun et al., Report LPC Caen 94-14 (1994), unpublished;
J.C. Steckmeyer et al., Phys. Rev. Lett. **76** (1996) 4895.

[13] J. Péter et al., Nucl. Phys. **A593** (1995) 95.

[14] R. Dayras et al., DAPNIA/SPhN-97-14, Contribution VII, Conference franco-japonais, Dogashima, October 1996.

[15] Y. Larochelle et al., Phys. Rev. C **55** (1997) 1869.

[16] P. Pawłowski et al., accepted for publication in Phys. Rev. C.

[17] D. Durand and B. Tamain, LPC Caen/LPCC 96-16, International Summer School, Les Houches (France) August 1996.

[18] J.C. Angélique et al., Nucl. Phys. **A614** (1997) 261.

[19] J. Tõke et al., Phys. Rev. C **56** (1997) 1683.

[20] M.B. Tsang and P. Danielewicz, preprint MSUCL-1069 (1997).

[21] A. Del Zoppo et al., Phys. Rev. Lett. **75** (1995) 2288.

[22] J. Pouthas et al., Nucl. Inst. and Meth. A **357** (1995) 418; A **369** (1996) 222;
J.C. Steckmeyer et al. Nucl. Inst. and Meth. A **361** (1995) 472.

[23] A. Wieloch et al., Zeit. Phys. **A359** (1997) 345.

[24] D. Durand, code SIMON in preparation.

## Figure captions

**Fig. 1** Elementary probability $1/p$ (panels a,b) and number of drawings $m$ (panels c,d) as a function of $1/\sqrt{E_t}$. $E_t$ denotes:
a,c) total transverse energy of all charged-particles and fragments,
b,d) transverse energy of LCP's,$E_{t,LCP}$: full and empty squares;
$E_{t,LCP}$ plus mean transverse energy of IMF's: full triangles;
$E_{t,LCP}$ plus randomized transverse energy of IMF's: full stars.
The solid line in panel a is a fit with an exponential dependence of $1/p$ on $1/\sqrt{E_t}$ while the other lines are to guide the eye. Open symbols indicate negative values of $1/p$ and $m$ . The solid lines from a) and c) are redrawn in b) and d), respectively, to facilitate comparison.

**Fig. 2** Distributions of IMF's c.m. velocity component along the beam for four bins ($\pm 40$ MeV) in $E_t$. In each panel the two numbers give the center of $E_t$ bin and the mean $N_{IMF}$ per event. The solid curves correspond to the case where the heaviest product, **when within** $3 \leq Z \leq 20$, was eliminated while for the dashed curves case this heaviest product was taken into account. The thin arrows in each panel represent the velocity of the target and projectile, while the broad ones indicate the mean value and FWHM of the velocity distribution of the QP residue. The black circles and the right-hand scale correspond to the average transverse energy per parallel velocity bin for Z=2 particles.

**Fig. 3** a) Average IMF transverse energy $< E_{t,IMF} >$ as a function of the LCP transverse energy $E_{t,LCP}$ for the indicated IMF multiplicities.
b) IMF transverse energy distributions for the indicated IMF multiplicities.

**Fig. 4** $|1/p|$ (panel a) and $|m|$ (panel b) as a function of $1/\sqrt{E_x}$ obtained from the simulation of the decay of a single thermalised source. $E_x$ denotes:
- the true thermal energy, $E^*$, of the source: open diamonds. $E^*$ was divided by 4 to facilitate comparison with the other prescriptions.
- the LCP transverse energy: solid and open squares,
- the total transverse energy of charged products: solid and open circles.
The solid line in panel a results from a fit while the other lines are to guide the eye. Open symbols denote negative values of $1/p$ and $m$.

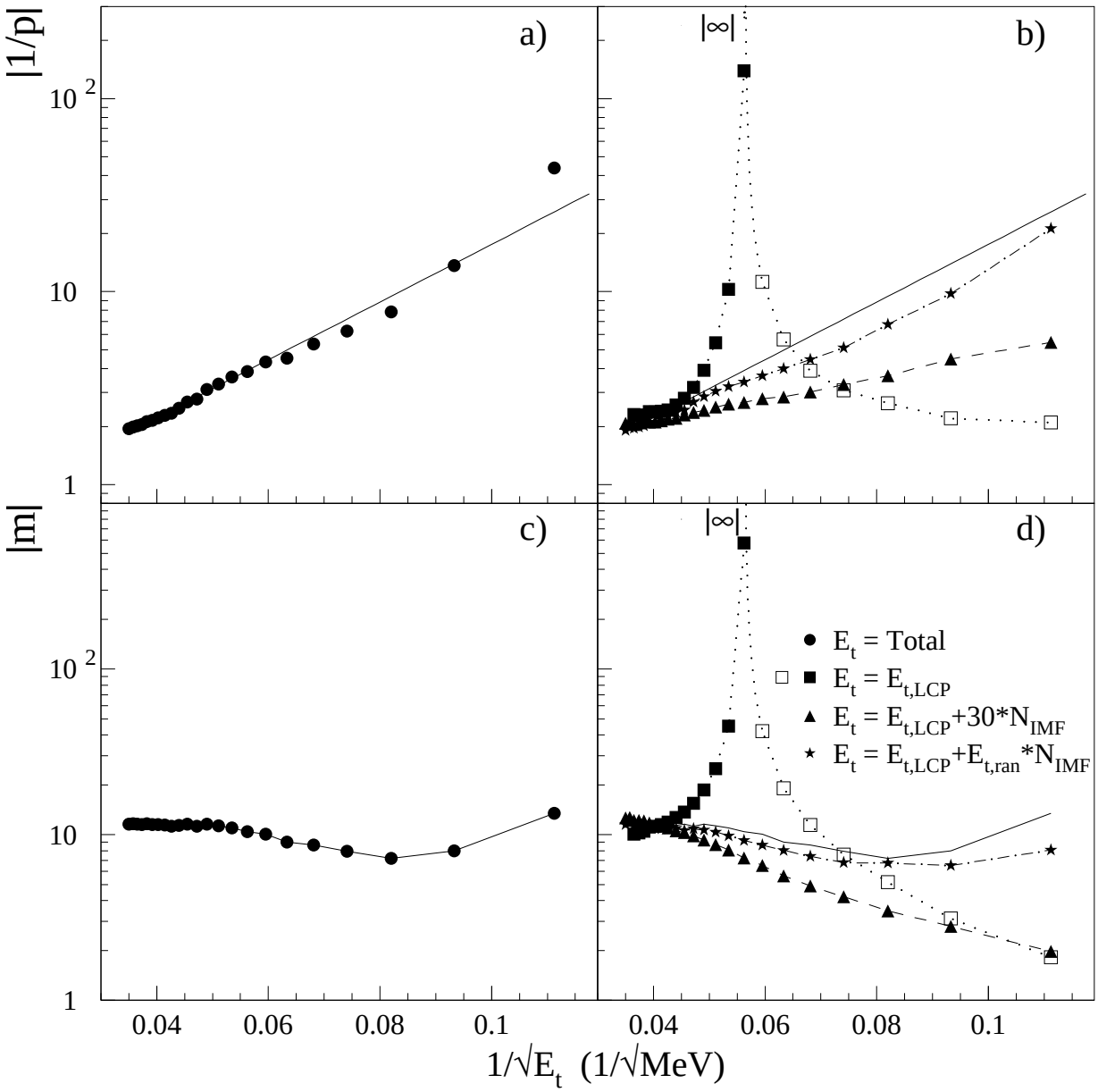
a)
b)
c)
d)
|1/p|
|m|
|∞|
|∞|
10 2
10
1
10 2
10
1
0.04
0.06
0.08
0.1
0.04
0.06
0.08
0.1
1/√E_t (1/√MeV)
E_t = Total
E_t = E_t,LCP
E_t = E_t,LCP+30*N_IMF
E_t = E_t,LCP+E_t,ran*N_IMF

**figure 1**

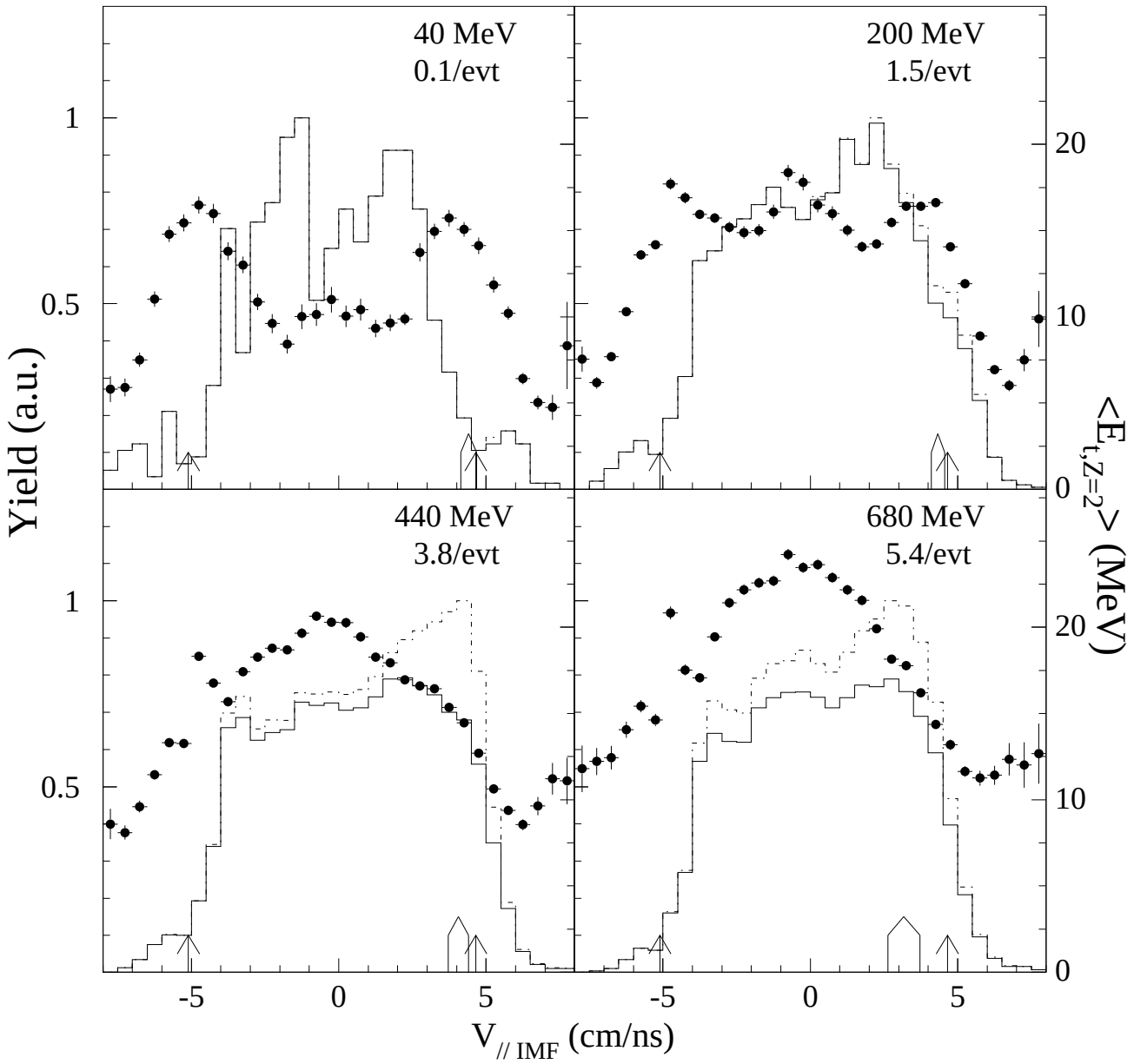
40 MeV
0.1/evt
200 MeV
1.5/evt
440 MeV
3.8/evt
680 MeV
5.4/evt
Yield (a.u.)
<E_t,Z=2> (MeV)
V_// IMF (cm/ns)
1
0.5
20
10
0
-5
0
5

**figure 2**

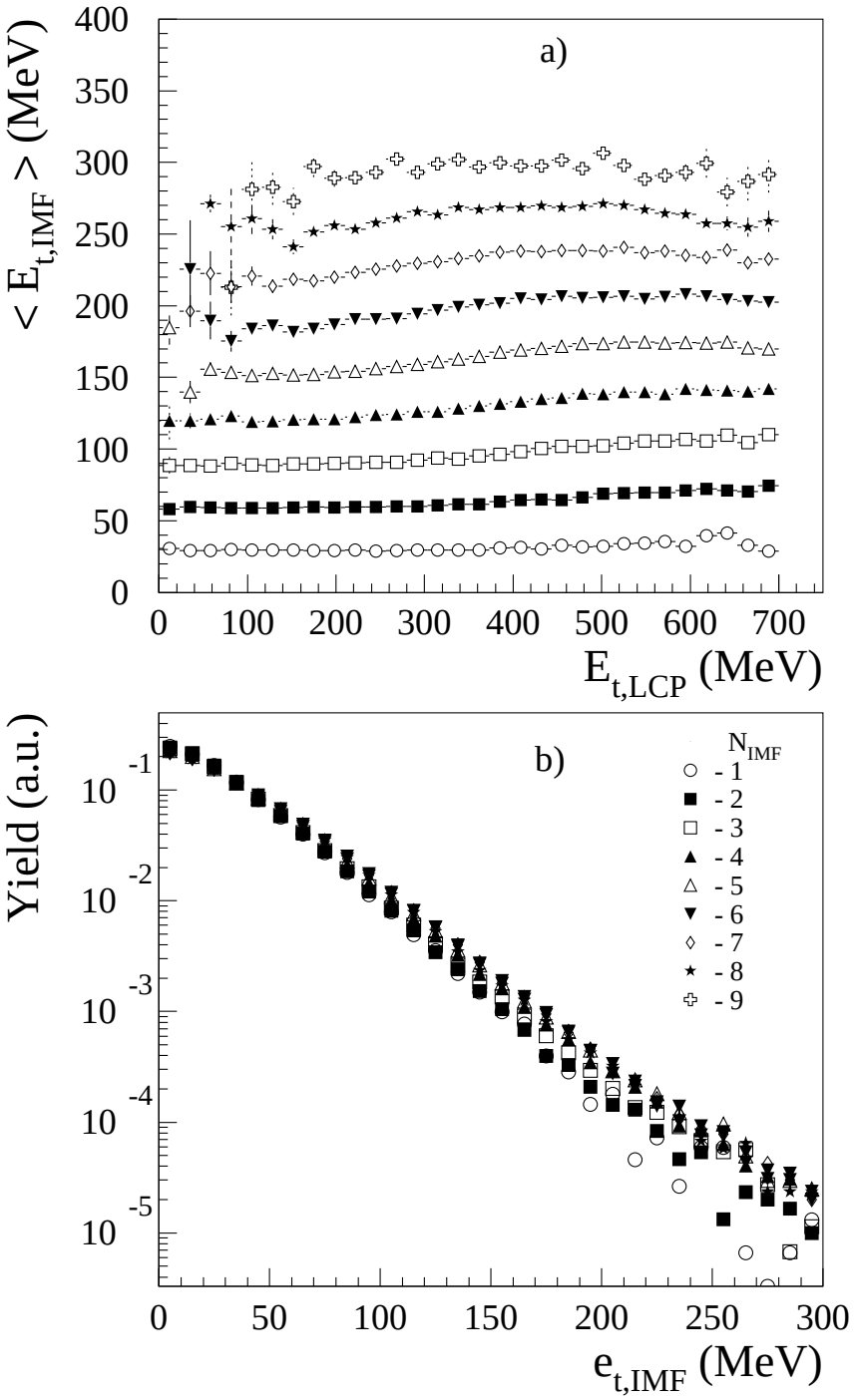


**figure 3**

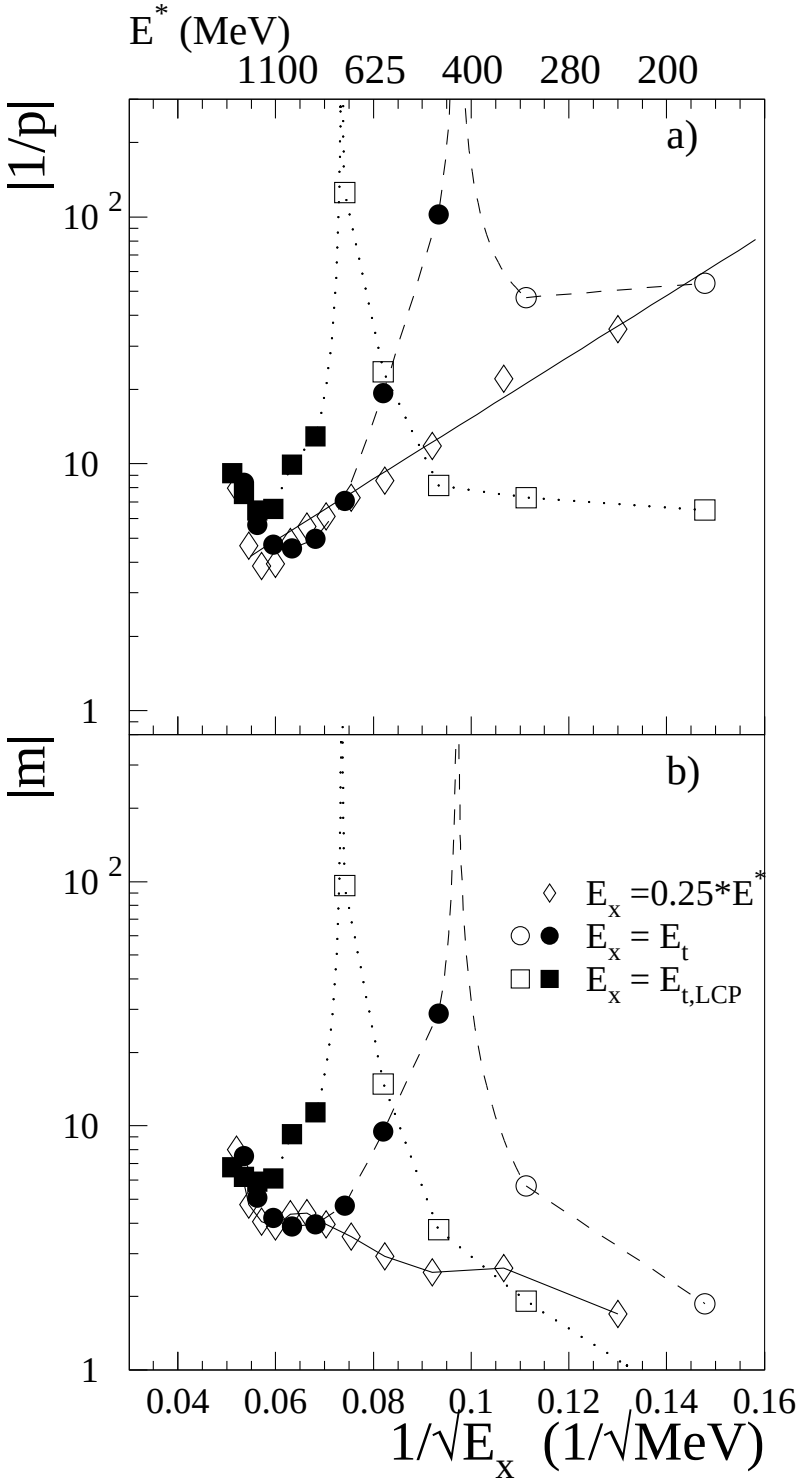
E* (MeV)
1100 625 400 280 200
a)
|1/p|
10 2
10
1
b)
|m|
10 2
10
1
E_x =0.25*E*
E_x = E_t
E_x = E_t,LCP
0.04 0.06 0.08 0.1 0.12 0.14 0.16
1/√E_x (1/√MeV)

**figure 4**